SEISMIC AND GEOPHYSICAL CHARACTERIZATION OF NORTHERN ASIA

Kevin G. Mackey[1], Hans E. Hartse[2], Kazuya Fujita[1], Michael E. Pasyanos[3], and Michael L. Begnaud[2]

Michigan State University[1], Los Alamos National Laboratory[2], and Lawrence Livermore National Laboratory[3]

Sponsored by the National Nuclear Security Administration

Award Nos. DE-AC52-09NA29323[1], DE-AC52-06NA25396[2], and DE-AC52-07NA27344[3]
Proposal No. BAA09-19

ABSTRACT

We are continuing our research effort to improve the seismic calibration of northern Asia. In conjunction with colleagues from the Geophysical Survey of Russia, we conducted a noise survey and station installation in the Amur region, south of the city of Blagoveschensk. For the noise study, four locations, each separated by about one kilometer, were surveyed. The general region was found to be rather noisy, with higher frequencies (1-20 Hz) coinciding approximately to the high noise model, while lower frequencies are approximately between the high and low noise models. The noise is not likely anthropogenic, but may be associated with the large Amur river about 10km distant. We conducted a winter deployment of 9 temporary stations in the vicinity of the Susuman mining district to collect data to develop a locally calibrated set of ground truth (GT) criteria. The current GT criteria using P arrivals for teleseismic events established by Bondar is generally not applicable to the eastern Russia data set as most arrivals are secondary Pg and Sg (Lg onset) time picks. The deployed temporary stations supplement 6 permanent stations, and encircle the mining region at varying distances out to about 250km. During the course of the deployment, we recorded 6 mine blasts with yields ranging up to 70 tons. An additional station was deployed at the explosion sites to record the exact origin time and location. Following our earlier work to determine new GT locations for Yakutian peaceful nuclear explosions (PNEs), we are now investigating how the new locations influence velocity model determination. Using arrivals from both the eastern Russia regional as well as teleseismic seismic stations we have estimated new origin times for Crystal, Neva-1, Neva-2-1, and Neva-2-3. We used the 3-d velocity model and locator under development at SNL and LANL while holding the new PNE latitude and longitude information fixed. We find differences between the time-distance relationships for Crystal and for the Neva shots using our new information and the Sultanov information. Differences are most apparent from Crystal, for which the location has been revised by over 40 km. Simple time-distance regressions to find Pg and Lg velocity for the Neva data at distances out to 1500 km show a slight velocity increase (Pg from 6.10 km/s to 6.15 km/s and Lg from 3.48 km/s to 3.51 km/s) by using the new GT locations compared to those of Sultanov. On other work, we continue our comprehensive seismic database efforts for eastern Russia, adding events with associated bulletin information (phase arrival times, amplitude measurements, etc.).

Report Documentation Page

Form Approved
OMB No. 0704-0188

1. REPORT DATE **SEP 2011**	2. REPORT TYPE	3. DATES COVERED **00-00-2011 to 00-00-2011**
4. TITLE AND SUBTITLE **Seismic and Geophysical Characterization of Northern Asia**		5a. CONTRACT NUMBER
		5b. GRANT NUMBER
		5c. PROGRAM ELEMENT NUMBER
6. AUTHOR(S)		5d. PROJECT NUMBER
		5e. TASK NUMBER
		5f. WORK UNIT NUMBER
7. PERFORMING ORGANIZATION NAME(S) AND ADDRESS(ES) **Michigan State University,East Lansing,MI,48824**		8. PERFORMING ORGANIZATION REPORT NUMBER
9. SPONSORING/MONITORING AGENCY NAME(S) AND ADDRESS(ES)		10. SPONSOR/MONITOR'S ACRONYM(S)
		11. SPONSOR/MONITOR'S REPORT NUMBER(S)
12. DISTRIBUTION/AVAILABILITY STATEMENT **Approved for public release; distribution unlimited**		
13. SUPPLEMENTARY NOTES **Published in the Proceedings of the 2011 Monitoring Research Review - Ground-Based Nuclear Explosion Monitoring Technologies, 13-15 September 2011, Tucson, AZ. Volume I. Sponsored by the Air Force Research Laboratory (AFRL) and the National Nuclear Security Administration (NNSA). U.S. Government or Federal Rights License**		

14. ABSTRACT

We are continuing our research effort to improve the seismic calibration of northern Asia. In conjunction with colleagues from the Geophysical Survey of Russia, we conducted a noise survey and station installation in the Amur region, south of the city of Blagoveschensk. For the noise study, four locations, each separated by about one kilometer, were surveyed. The general region was found to be rather noisy, with higher frequencies (1-20 Hz) coinciding approximately to the high noise model, while lower frequencies are approximately between the high and low noise models. The noise is not likely anthropogenic, but may be associated with the large Amur river about 10km distant. We conducted a winter deployment of 9 temporary stations in the vicinity of the Susuman mining district to collect data to develop a locally calibrated set of ground truth (GT) criteria. The current GT criteria using P arrivals for teleseismic events established by Bondar is generally not applicable to the eastern Russia data set as most arrivals are secondary Pg and Sg (Lg onset) time picks. The deployed temporary stations supplement 6 permanent stations, and encircle the mining region at varying distances out to about 250km. During the course of the deployment, we recorded 6 mine blasts with yields ranging up to 70 tons. An additional station was deployed at the explosion sites to record the exact origin time and location. Following our earlier work to determine new GT locations for Yakutian peaceful nuclear explosions (PNEs), we are now investigating how the new locations influence velocity model determination. Using arrivals from both the eastern Russia regional as well as teleseismic seismic stations we have estimated new origin times for Crystal, Neva-1, Neva-2-1, and Neva-2-3. We used the 3-d velocity model and locator under development at SNL and LANL while holding the new PNE latitude and longitude information fixed. We find differences between the time-distance relationships for Crystal and for the Neva shots using our new information and the Sultanov information. Differences are most apparent from Crystal, for which the location has been revised by over 40 km. Simple time-distance regressions to find Pg and Lg velocity for the Neva data at distances out to 1500 km show a slight velocity increase (Pg from 6.10 km/s to 6.15 km/s and Lg from 3.48 km/s to 3.51 km/s) by using the new GT locations compared to those of Sultanov. On other work, we continue our comprehensive seismic database efforts for eastern Russia, adding events with associated bulletin information (phase arrival times, amplitude measurements, etc.).

15. SUBJECT TERMS

16. SECURITY CLASSIFICATION OF:			17. LIMITATION OF ABSTRACT	18. NUMBER OF PAGES	19a. NAME OF RESPONSIBLE PERSON
a. REPORT **unclassified**	b. ABSTRACT **unclassified**	c. THIS PAGE **unclassified**	**Same as Report (SAR)**	**10**	

Standard Form 298 (Rev. 8-98)
Prescribed by ANSI Std Z39-18

OBJECTIVES

The objectives of this project are to characterize the seismicity and geophysical parameters of northern Asia.

RESEARCH ACCOMPLISHED

Station Installation and Noise Survey in Amur

In cooperation with the Geophysical Survey of Russia, we conducted a noise survey and seismic station installation in the Amur region of eastern Russia (Figure 1). The station is located in the classroom building of the Muraviovka Nature Preserve about 45 km south of the city of Blagovashensk, Russia. The station site is situated on a sand/gravel bluff overlooking the floodplain of the Amur River. The station consists of mid-period SM3-kv seismometers (three individual components) that are digitized, with data being transmitted to Obninsk through the cellular phone network. The noise survey conducted in the region utilized a Guralp CMG6T broadband seismometer that was deployed at the station site and three nearby locations. Each location was separated by approximately 1 km to quantify local sources and obtain a better estimate of the regional noise levels. Although we generally expected low noise levels because the sites are far from populations and there was almost no vehicular traffic on or around the farmland in the area, we found noise levels to be around the high noise model, similar to the reference station in Obninsk that is located near a large town (Figure 2). The source of the noise is not apparent, though may relate to the nearby Amur River. Depending on the overall quality of the recordings from the station, the long term status of the deployment at the site remains to be determined.

Figure 1. Left – Station deployment site at Muraviovka Park (red) and noise survey locations (pink) in the Amur region of eastern Russia. The small red square on the inset shows the location. Center – Station installation. Right – Station building overlooking the floodplain of the Amur River.

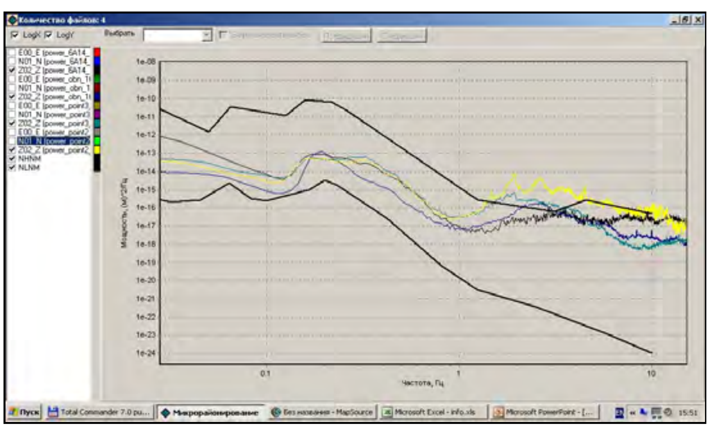

Figure 2. Noise survey in the region of Muraviovka Park in the Amur region of eastern Russia. The vertical component of three survey locations (yellow, black, and teal) are compared to the station at Obninsk (dark blue).

Improving GT Criteria for Eastern Russia

We are developing an improved set of GT determination criteria for Eastern Russia, which do not typically lend themselves to the Bondár et al. (2004) criteria. The Bondár et al. (2004) criteria do not accept Sg phases nor Pg phases available beyond the Pg/Pn crossover distance. Such Pg and Sg phases comprise the bulk of our database and are of high quality. We have recently undertaken fieldwork in eastern Russia to develop the new GT criteria for the region using mine blasts and temporary station deployments. In April-May 2011 we deployed 9 temporary seismic stations in the Susuman mining region of eastern Russia (Figure3) and recorded 6 explosions ranging up to 70 tons (Figure 4). The temporary sites supplemented the regions permanent stations and were arranged to maximize statistical possibilities in analysis. Data have not yet been analyzed. Similar fieldwork, but with a less than ideal station distribution, was conducted in 2004, when it was generally found that that events could be located at the GT-3 level using multiple phases and a locally calibrated travel-time curve, but with a poor distribution of stations (Mackey et al., 2004).

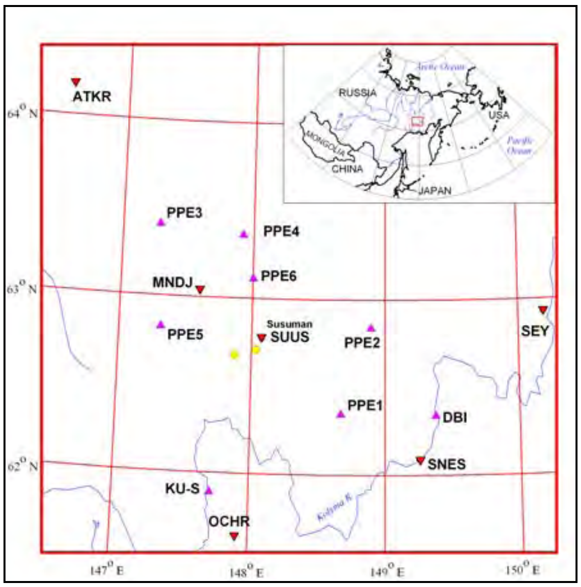

Figure 3. Left – Temporary (pink) and permanent (red) seismic stations deployed in the vicinity of the Susuman mining district. Six GT explosions ranging up to 70 tons were recorded that originated from two of the mines in the region (yellow). Right – Station deployment PPE1 consisting of SM3 short period seismometers deployed on ice.

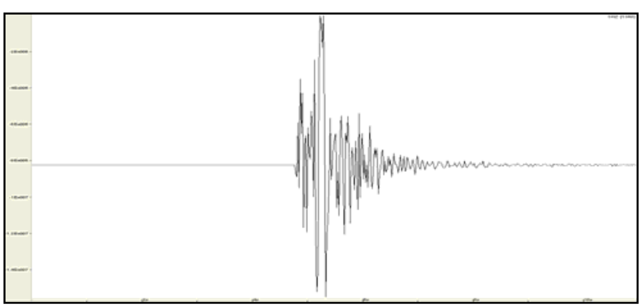

Figure 4. GT-0 explosion seismogram from April 21, 2011 as recorded at the mine site.

New Estimation of PNE Origin Times and Velocities

We have also been collecting additional phase data from the PNEs, especially from regional stations. Using these data and other regional and teleseismic arrival times held by LANL, we have estimated new origin times for the relocated PNEs (Table 1). We used the 3-d velocity model and locator under development at SNL and LANL (Hipp et al., 2011) while holding the new PNE latitude and longitude information fixed. Figures 5 and 6 show

differences between the time-distance relationships for Crystal and for the Neva shots, respectively, using our new parameters and the Sultanov et al. (1999) information. As the Crystal location has been revised by over 40 km, differences are most apparent. By comparing the simple time-distance regressions, we can calculate Lg and Pg velocity for the Neva data at distances out to 1500 km. For the new GT location and origin time, we find Pg and Lg velocities to 6.15 km/sec and 3.51 km/sec respectively, slightly faster than 6.10 km/sec and 3.48 km/sec respectively when using the source parameters from Sultanov et al. (1999). We will continue to investigate how the new GT information influences velocity model estimation.

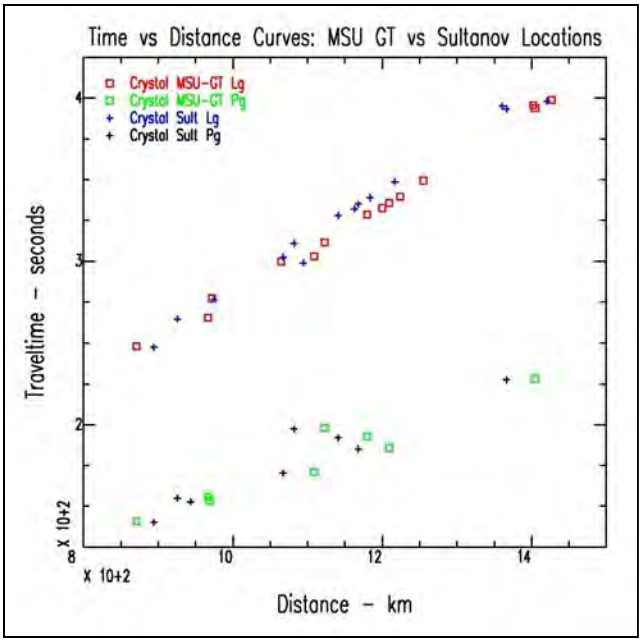

Figure 5. Comparison of travel times using our epicentral coordinates and those from Sultanov et al. (1999) for PNE Crystal.

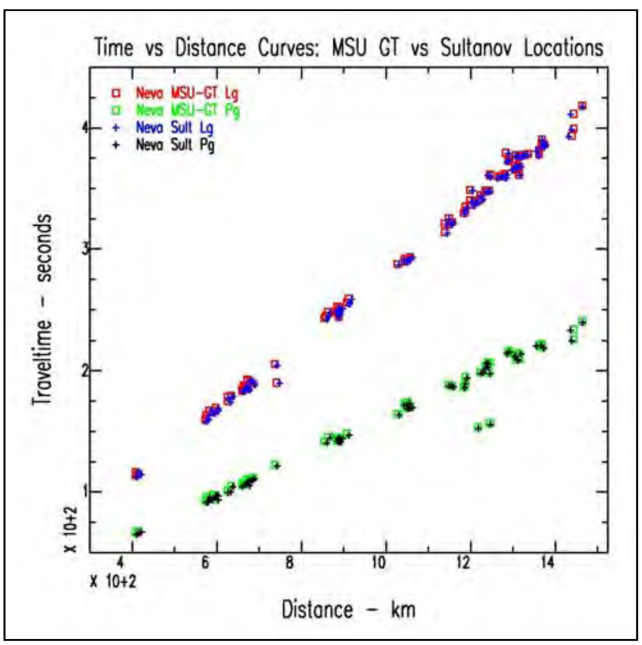

Figure 6. Comparison of travel times using our epicentral coordinates and those from Sultanov et al. (1999) for three of the Neva PNEs.

Table 1. Revised origin times of selected Yakutian PNEs

PNE	Latitude (N)	Longitude (E)	Date	Recalculated Origin Time
Crystal	66.4573	112.3989	1974 10 02	01 00 00.43
Oka	61.4608	112.8592	1976 11 05	03 59 59.22
Craton-4	63.6800	125.5267	1978 08 09	18 00 00.30
Kimberlite-4	61.7997	122.4161	1979 08 12	17 59 59.79
Craton 3	65.9254	112.3330	1978 08 24	18 00 00.07
Vyatka	61.5565	112.9922	1978 10 07	23 59 59.46
Neva 1	61.5006	112.9110	1982 10 10	04 59 59.60
Neva 2-1	61.4317	112.8860	1987 07 06	23 59 59.37
Neva 2-3	61.4266	112.8879	1987 08 12	01 29 59.36

Energy Magnitude (M_e) and Energy Class (K) Relations

Since 1987, the US Geological Survey has calculated the radiated energy, E_S, from the energy spectral density of broadband P-waves (Boatwright and Choy, 1986). The Energy magnitude is then calculated using the relationship (Choy and Boatwright, 1995),

$$M_e = 2/3 \log E_S - 2.9$$

where energy is in Newton-meters.

Since K-class is also supposed to estimate radiated energy (in joules; Rautian et al., 2007), a direct correlation should exist between M_e and K,

$$M_e = 0.666K - 2.933.$$

We have tabulated M_e and K values (K_R in continental Asia, K_S or K_F in the subduction zones of the Far East) and the correspondence is fairly good in the Far East, Altai-Sayan, Kopetdag, and the Caucasus (Figure 7), although there are offsets which may reflect differing stress drops and variation in the frequency of energy radiated (Figure 7) The regression for the Kamchatka data is

$$M_e = 0.6564\,K - 2.9358$$

and

$$M_e = 0.6927\,K - 4.5603$$

for Kopetdag, both of which are extremely close to expected relationship. The Caucasus have a similar slope but a different intercept. The K-class determinations from the 1980s and 1990s relied primarily on Soviet SKM and SM-3 seismometers that were recorded on photopaper. Because the stations were generally uniform, stations were consistently calibrated across the country, and standards of analysis were similar. Since the break-up of the Soviet Union, many of the seismic networks have converted to digital recording. Unfortunately, it appears that the conversion to digital recording of old Soviet sensors and the introduction of many new instruments and analysis techniques of digital data may have resulted in an overall degradation of K-class determination. Nomograms for K-class determination have not been developed for new instruments and recording systems. Figure 8 shows a plot of actual period measurements from station Stekolnyi in the Magadan region. Older measurements made using SM-3

instruments recorded on photopaper show a wide range of periods measured for K-class determinations, likely reflective of actual dominant period of the highest amplitude waves in the seismogram. Newer analysis of digital waveforms from Stekolnyi using the same set of SM-3 seismometers shows a much narrower band of shorter period measurements used in determining K-class values. The narrow frequency band is likely the result of frequency and amplitude measurements taken after the waveforms have been band-pass filtered. The poorly calibrated nature of many stations and post-filter measurements may result in unreliable K-class determinations and thus an unreliable relationship between K and M_e. It is most likely that the level of such problems varies considerably, and problems may not exist in all networks. We are continuing to understand and relate the frequency-amplitude measurements utilized in the Former Soviet Union networks for K-class determination.

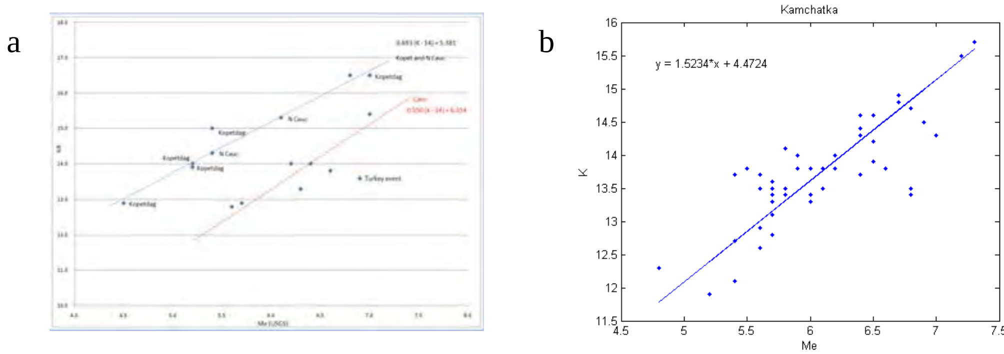

Figure 7. Relationship between Energy Magnitude (M_e) and Energy Class (K) for the a) Caucasus (red line) and Kopetdag (blue line) regions and b) Kamchatka.

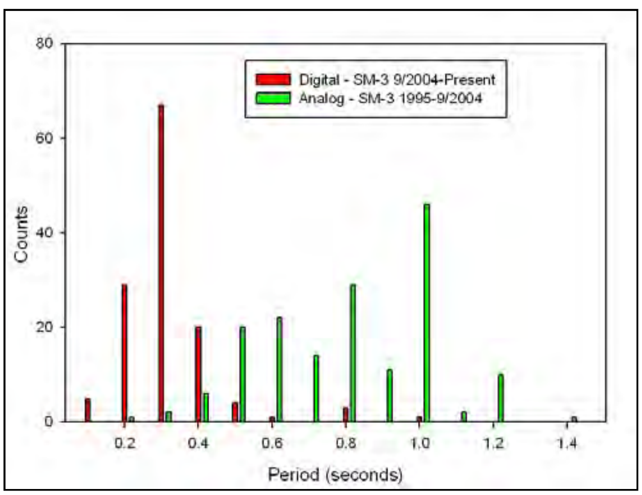

Figure 8. Periods used to determine K-class values using data from station Stekolnyi, in the Magadan network. Data from the digital era shows most measurements in a narrow short period band, a result of analysis after filtering of data. Data shown are representative of the time intervals indicated.

Improvement of Surface Wave Studies for Siberia

Figure 9 shows a pair of dispersion maps for Siberia. The group velocity maps are derived from the global maps being developed for the LITHO1.0 model (see Masters et al., 2011 these proceedings). The high resolution of the model results from the development of a new, extremely large global datasets of group velocities using a new, efficient measurement technique that employs cluster analysis (Ma et al., 2011). Maps have been developed for Rayleigh and Love waves from 10 mHz to 40 mHz. The 40 mHz dispersion map does a good job of differentiating

between oceanic and continental crust. One interesting anomaly is a region of high velocity along the coast of the Arctic Ocean. Very little independent data exist on the crustal structure or composition in this area. The 10 mHz data, sampling at greater depth, quite accurately maps the tectonically active and younger regions as lower velocity zones, while regions associated with old cratons show high velocities, as would be expected.

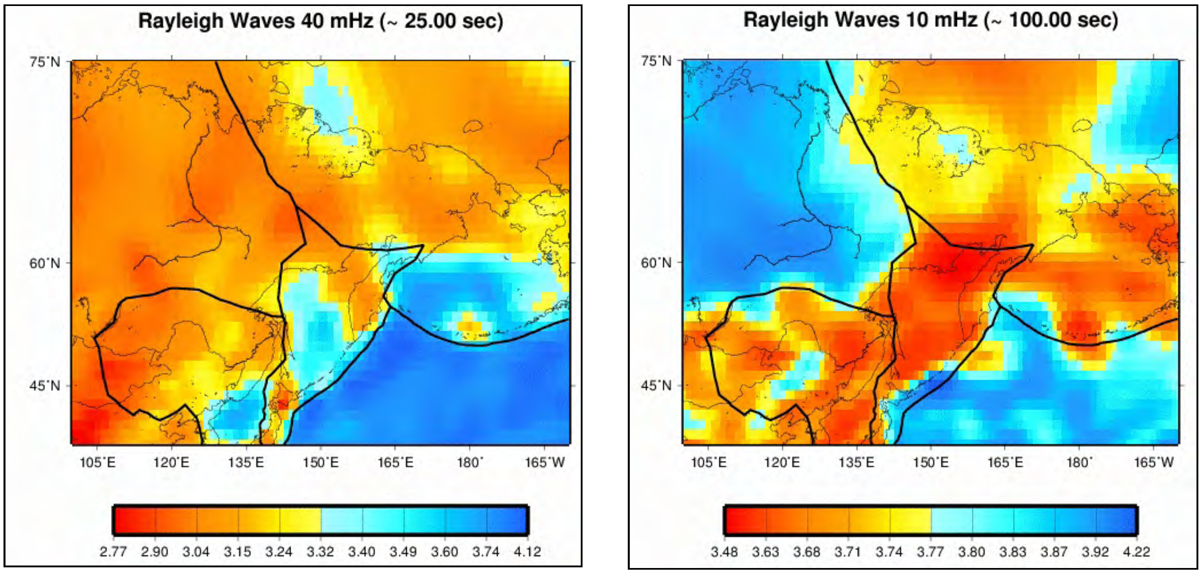

Figure 9. Surface wave dispersion maps for Siberia. The 40 mHz map at left is generally sampling the crust, while the 10 mHz map at right is sampling velocities at greater depth.

Altai Sayan Network Additions to the Database

We continue the development of our seismicity database for eastern Russia. Specifically for this project, we are focusing expansion further west to include the Altai-Sayan seismic network. A sufficient number of hypocenters are now in the database (approximately 20,000) to show statistically that the database is contaminated with explosions. Following the same procedures as in previous studies (Mackey and Fujita, 1999, Mackey et al, 2002, and Mackey et al., 2003), a qualitative estimate of the level of explosion contamination and levels of natural seismicity can be obtained by examining the spatial and temporal characteristics of earthquakes located by the regional networks. The study area was divided into cells in which the percentages of daytime earthquakes are calculated. Cells containing fewer than eight events were not considered to be statistically significant, and were not analyzed. The 12 hour local "day" has been shifted according to time zones. Light blue areas in Figure10 represent regions where seismicity is roughly balanced between night and day, and dark blue areas are those in which seismicity is concentrated during local night (>65%). There are several areas of nighttime-biased seismicity, most of which are in seismically less active regions and away from seismic stations. This is not unexpected since almost all seismic stations in the area are located in populated areas, and thus have lower cultural noise during the night. Pink areas on Figure 3 represent regions where more than 65% of the seismicity occurs during local "day". Many of the regions with predominantly daytime events are found in discrete clusters or trends of seismicity, most of which can be associated with mining or construction related blasting.

In addition to event locations, our database will also be expanded with phase data from the network. Thus far, we have entered phase data for events larger than K-class 9.5 primarily from 1983 through 1986. Total, this represents about 5,100 raypaths, and already provides good coverage of much of the network (Figure 11). Although the formal boundaries of the Altai-Sayan network include parts of Mongolia, China, and Kazakhstan, it appears that only the Baikal network data are included in the Altai-Sayan seismicity bulletin. A plot of travel-time curves of the Altai Sayan network shows a dominance of Pg and Sg phases out to distances of greater than 1000km, suggesting good transmission of these phases in the crust (Figure 12). The scatter in the travel-time curves indicates that hypocenters can probably be improved by using a better calibrated velocity model.

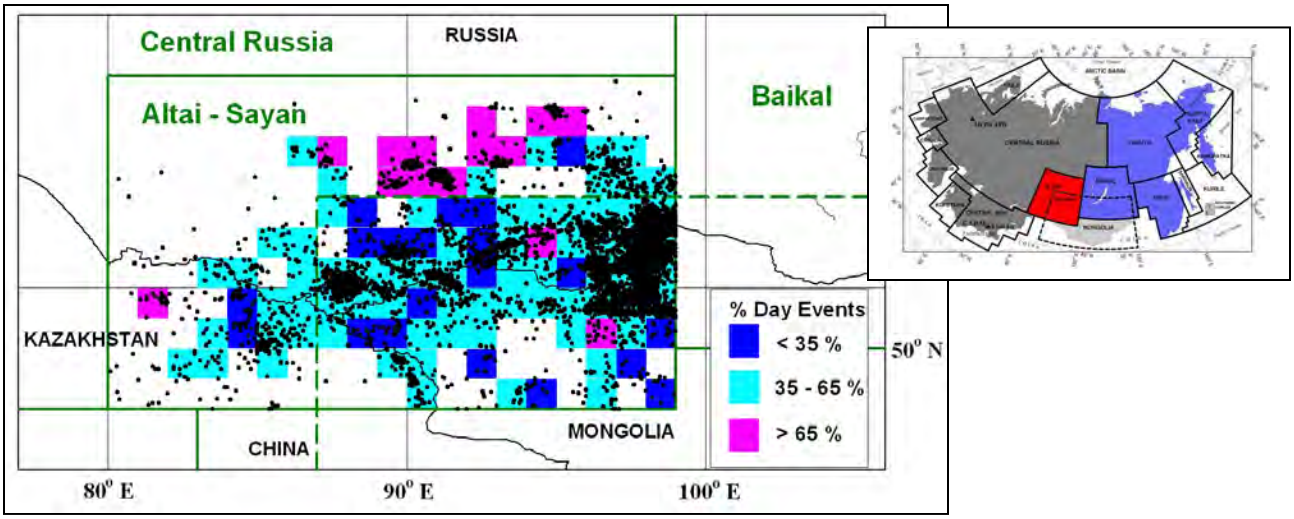

Figure 10. Seismicity of the Altai-Sayan network showing percentages of daytime events by cell. Explosion contamination of the seismicity catalog is suspected where cells are pink (> 65% of the events occur during local daytime). Data depicted are more complete in the eastern edge of the network due to overlap of locations from the Baikal network. Events outside the Altai-Sayan network are not shown. The inset shows the location of the Altai Sayan Network in red and previously compiled portions of the database in blue.

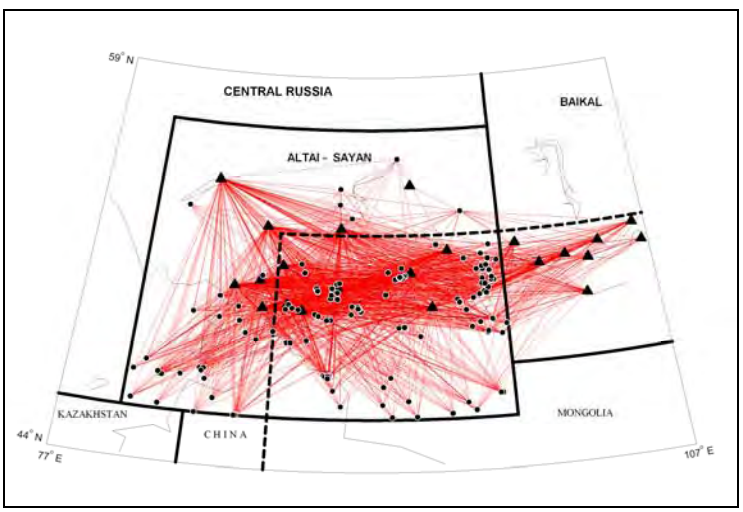

Figure 11. Raypath coverage of Altai-Sayan network phase data to the MSU-LANL Siberia database, showing approximately 5,100 paths. Triangles are seismic stations and circles are events.

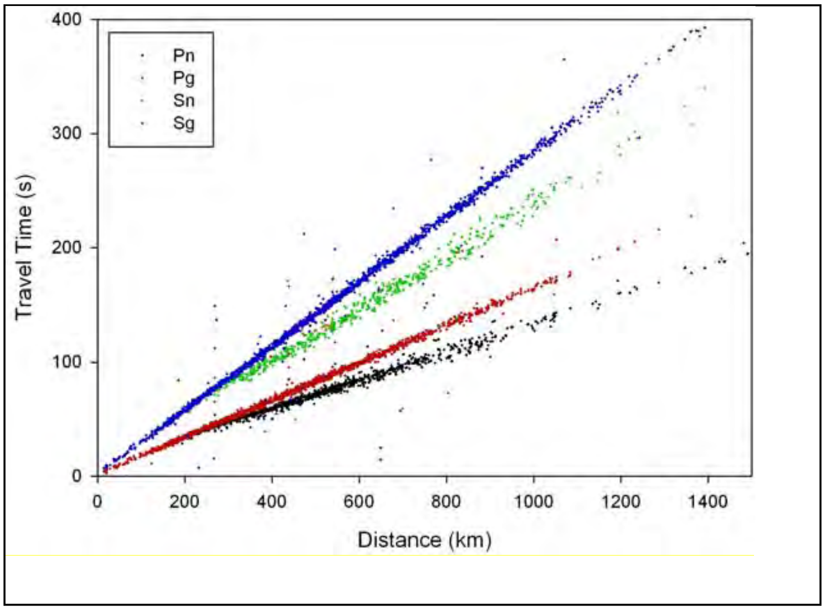

Figure 12. Travel-time curves of the Altai-Sayan network representing data primarily from events larger than K-class 9.5 between 1983 and 1986. Note that the dominant phases reported are Pg and Sg.

CONCLUSIONS AND RECOMMENDATIONS

This project will improve our knowledge on many geophysical aspects of northern Asia. As summarized here, this is inclusive of field deployments, seismic characterization, surface wave tomography, analysis of PNE data, improving the GT categorization of events, event energy and magnitude estimates, and database expansion.

ACKNOWLEDGEMENTS

We would like to thank Peter Bormann and Anthony Kendall for assistance on this project.

REFERENCES

Boatwright, J. L., and G. L. Choy (1986). Teleseismic estimates of the energy radiated by shallow earthquakes, *J. Geophys. Res.* 91: 2095–2112.

Bondár, I., S. C. Myers, E. R. Engdahl, and E. A. Bergman (2004). Epicentre accuracy based on seismic network criteria: *Geophys. J. Int.* 156: 483–496.

Choy, G. L., and J. L. Boatwright (1995). Global patterns of radiated seismic energy and apparent stress Global patterns of radiated seismic energy and apparent stress, *J. Geophys. Res.* 100: 18,205–18,228.

Hipp, J.R., A.V. Encarnacao, S. Ballard, C.J. Young, M.C. Chang, W.S. Phillips, and M.L. Begnaud (2011). Calculating path-dependent travel time prediction variance and covariance for the SALSA3D global tomographic P-velocity model, *Seismol. Res. Lett.* 82: 280.

Ma, Z., T.G. Masters, G. Laske and M.E. Pasyanos (in prep.). A new global Rayleigh wave group velocity dataset for constraining crust and upper mantle properties.

Mackey, K.G., and K. Fujita, 1999. The northeast Russia seismicity database and explosion contamination of the Russian earthquake catalog, in *Proceedings of the 21st Seismic Research Symposium: Technologies for Monitoring the Comprehensive Nuclear-Test-Ban Treaty*, LA-UR-99-4700, Vol.1, pp.151–161.

Mackey, K. G., K. Fujita, L. K. Steck, and H. E. Hartse (2002). Seismic regionalization in northeast Russia, *in Proceedings of the 24th Seismic Research review - Nuclear Explosion Monitoring: Innovation and Integration*, LA-UR-02-5048, Vol. 1, pp. 107–116.

Mackey, K. G., K. Fujita, L. Gounbina, B. Koz'min, V. Imaev, L. Imaeva, and B. Sedov (2003). Explosion contamination of the northeast Siberian seismicity catalog: implications for natural earthquake distributions and the location of the Tanlu fault in Russia, *Bull. Seismol. Soc. Am.* 93: 737–746.

Mackey, K. G., K. Fujita, H. E. Hartse, and L. K. Steck (2004). Seismic Regionalization Research in Northeast Russia, *in Proceedings of the 26th Seismic Research Review - Trends in Nuclear Explosion Monitoring*, LA-UR-04-5801, Vol. 1, pp. 92–101.

Rautian, T., V. Khalturin, K. Fujita, K. Mackey, and A. Kendall (2007). Origins and methodology of the Russian energy K-class system and its relationship to magnitude scales: *Seismol. Res. Lett.* 78: 579-590.

Sultanov, D. D., J. R. Murphy, and K. D. Rubinstein (1999). A seismic source summary for Soviet peaceful nuclear explosions: *Bull. Seismol. Soc. Am.* 89: 640–647.